

## Radiation Dry Bias Correction of Vaisala RS92 Humidity Data and Its Impacts on Historical Radiosonde Data

JUNHONG WANG

*National Center for Atmospheric Research,\* Boulder, Colorado, and Department of Atmospheric and Environmental Sciences, University at Albany, State University of New York, Albany, New York*

LIANGYING ZHANG

*National Center for Atmospheric Research,\* Boulder, Colorado*

AIGUO DAI

*Department of Atmospheric and Environmental Sciences, University at Albany, State University of New York, Albany, New York, and National Center for Atmospheric Research,\* Boulder, Colorado*

FRANZ IMMLER

*European Commission, Brussels, Belgium*

MICHAEL SOMMER AND HOLGER VÖMEL

*GRUAN Lead Centre, Deutscher Wetterdienst, Lindenberg, Germany*

(Manuscript received 9 June 2012, in final form 24 September 2012)

### ABSTRACT

The Vaisala RS92 radiosonde is the most widely used type of sonde in the current global radiosonde network. One of the largest biases in the RS92 humidity data is its daytime solar radiation dry bias (SRDB). An algorithm [referred to as NCAR radiation bias correction (NRBC)] was developed to correct the SRDB based on a more complicated algorithm developed by the Global Climate Observing System (GCOS) Reference Upper-Air Network (GRUAN). The NRBC to relative humidity (RH) is a function of the measured RH and temperature, and the temperature solar radiation correction. The latter varies with pressure, season, and time of the day. The RH correction has a mean magnitude of about 2%–4% and 6%–8% in the lower–midtroposphere and upper troposphere, respectively. The NRBC is evaluated against the GRUAN-corrected RS92 data and the ground-based GPS-estimated precipitable water (PW). The corrected RH agrees with the GRUAN data within  $\pm 0.5\%$  on average, with standard deviations of about 1%–2% and 2%–6% in the lower–midtroposphere and upper troposphere, respectively. The NRBC leads to reduced mean biases, and better agreement with the GPS PW and its diurnal cycle. The NRBC has been applied to historical radiosonde data at 65 stations. The radiosonde humidity data, both with and without the NRBC, are homogenized using the method of Dai et al. (2011). The NRBC results in consistently elevated RHs throughout the whole record in the homogenized data. This could have a significant impact on global reanalysis products when they are assimilated into the reanalysis models. However, the NRBC has insignificant effects on the long-term trends as the correction is primarily for mean biases.

---

\* The National Center for Atmospheric Research is sponsored by the National Science Foundation.

---

Corresponding author address: Junhong (June) Wang, NCAR, 1850 Table Mesa Drive, Boulder, CO 80305.  
E-mail: junhong@ucar.edu

### 1. Introduction

Global radiosonde data represent an important resource for monitoring and understanding climate changes. These data provide the longest record (up to 60 years) of upper-air temperatures, humidity, and winds; and they have near-global coverage and high vertical resolution.

However, the application of the radiosonde records in climate studies is hampered, in part, by sensor-dependent errors that vary substantially over time and space. Among radiosonde-measured parameters, humidity is the most challenging because the sensor errors and biases in the approximately 18 types of radiosondes used in the global radiosonde network have yet to be characterized. Currently, the Vaisala RS92 radiosonde is the most popular sonde, used by ~30% of the global radiosonde stations.

The Vaisala RS92 radiosonde was first introduced in 2003. In contrast to its preceding version, Vaisala RS80, the RS92 is equipped with twin HUMICAPS designed to remove ice and water on the hygrometer through alternative heating of the two sensors. One drawback of this design is that the twin HUMICAPS prevent the use of a silver cap; found on the RS80s, it is meant to act as a radiation shield. Without the cap, solar radiation heating is more likely to occur, resulting in a dry bias to the measured relative humidity (RH). Vömel et al. (2007) were the first to quantify this radiation dry bias, and they found it to be on the order of 9% of the RH values at the surface and increasing to 50% at 15 km, where solar zenith angles are between 10° and 30° (in Costa Rica). They also developed a method to correct the bias. Subsequent studies have confirmed this dry bias in different regions and also presented different correction approaches (e.g., Cady-Pereira et al. 2008; Rowe et al. 2008; Nuret et al. 2008; Yoneyama et al. 2008; Agustí-Panareda et al. 2009; Miloshevich et al. 2009; Ciesielski et al. 2010). However, those correction methods were developed for specific regions, projects, or study periods; thus, they have not been tested for applicability to operational radiosonde data on a global scale.

These sensor-dependent errors and biases, together with other observational changes, often introduce non-climatic changes or inhomogeneities in historical records of humidity from radiosonde measurements (e.g., Dai et al. 2011). The radiosonde record needs to be homogenized before it can be used to estimate long-term humidity and water vapor trends. The homogenization involves first detecting stepwise change points in humidity time series or probability distribution functions (PDFs) and then adjusting the time series to remove the discontinuities. The adjustment requires a reference segment to which other segments are adjusted. The most recent segment is often selected to be the reference segment based on the assumption that newer measurements have improved data quality. Dai et al. (2011) developed a new approach to homogenize historical records of daily tropospheric dewpoint depression (DPD), using the most recent segment as the reference. Because mean biases still likely exist in the

latest measurements, the homogenized data will also likely contain mean biases, which could ultimately lead to systematic biases in other applications, such as when used in atmospheric reanalyses.

To address the shortcomings of the global operational networks for climate studies, and to ensure that future climate records are more useful than the records to date, the Global Climate Observing System (GCOS) program initiated a GCOS Reference Upper-Air Network (GRUAN) consisting of 30–40 sites worldwide (Seidel et al. 2009). GRUAN was developed during 2005–07 and is currently being implemented. The objectives of GRUAN are to provide long-term, high-quality upper-air climate records, to constrain and calibrate data from more spatially comprehensive global observing systems (including satellites) and to measure a large suite of correlated climate variables. One of the most important objectives of GRUAN is to collect reference observations. Each GRUAN reference observation is required to provide a comprehensive uncertainty analysis (Immler et al. 2010). Vaisala RS92s are launched regularly at 13 of the 15 current GRUAN candidate stations. Therefore, the GRUAN community decided to first develop data products from the Vaisala RS92 measurements, which include corrections for systematic errors and derivations of uncertainty for each data point and each parameter (Immler and Sommer 2011). The first GRUAN data product (GDP), Vaisala RS92-GDP, was released in June 2011 and is continually updated every day (Immler and Sommer 2011).

Given that Vaisala RS92 is the most widely used sonde in the current global radiosonde network and has been studied extensively to evaluate the performance of its humidity sensor, the focus of this study is on correcting the radiation dry bias in historical Vaisala RS92 global humidity data and investigating the impact of the corrections on homogenized long-term data records. In section 2, we describe the datasets used in this study and the algorithm for correcting the RS92 radiation dry bias. The algorithm is validated by comparing with the GRUAN algorithm and with atmospheric precipitable water (PW) estimated from ground-based GPS measurements in section 3. In section 4, we examine how the corrections affect the homogenization of the long-term (1960–2010) humidity time series. Conclusions are presented in section 5.

## 2. Data and bias-correction algorithm

### a. Radiosonde and GPS PW data

The long-term operational radiosonde dataset we used was derived by merging two radiosonde archives:

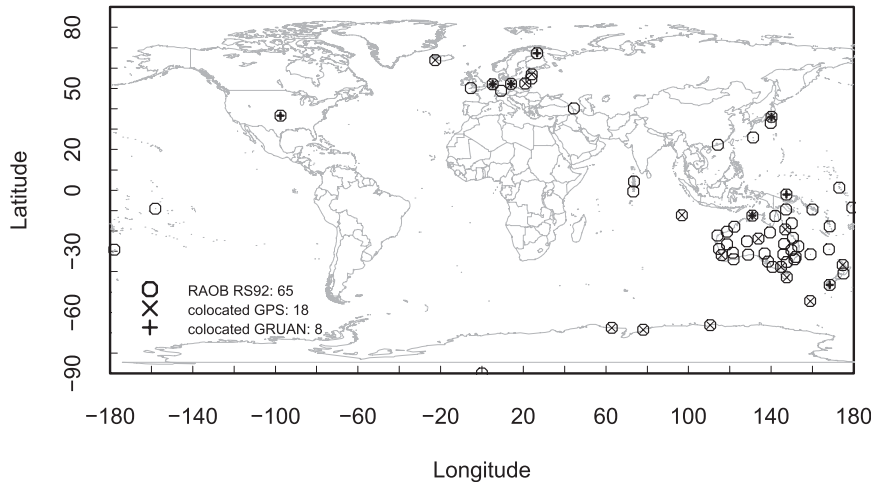


FIG. 1. Map of stations launching Vaisala RS92, collocated GPS stations, and GRUAN stations.

the Integrated Global Radiosonde Archive (IGRA; Durre et al. 2006) and the National Center for Atmospheric (NCAR) National Meteorological Center Automated Data Processing (NMC/ADP) radiosonde data archive (<http://rda.ucar.edu/datasets/ds351.0/>). We refer to this merged dataset as the NCAR Merged Radiosonde Archive (NMRA). The ADP data are compared with the IGRA to identify new stations and stations with additional data from ADP compared to the IGRA. A total of 99 new stations were added to the IGRA. Some stations in the IGRA had no moisture data for a number of years, and some had less than half of the moisture data in the ADP dataset. For these cases, the ADP records were used here. The total number of radiosonde stations in the NMRA varies from year to year. The period of record varies from station to station, with most of them extending from 1970 to the present. The data are available at standard and significant pressure levels. The IGRA metadata were updated and used to identify 65 stations that had accurate metadata on the date that launching the RS92 began, and those that had launched Vaisala RS92 sondes for more than one year (Fig. 1).

The RS92 GRUAN data product (RS92-GDP) version 001 is available at five sites; however, they contain more than one month of soundings only at three GRUAN sites in 2011, which are Lindenberg (Germany), Cabauw (Netherlands), and Tateno (Japan) (Fig. 1). Note that Fig. 1 shows all eight GRUAN sites located within 50 km of IGRA stations. We used the RS92-GDP to develop and validate our correction method described in section 2b. The RS92-GDP was created from the original DigiCORA III database files, and has been corrected for known systematic errors of all variables. The uncertainty of each variable for each data point, included in the RS92-GDP, was calculated using estimates of the calibration

uncertainty, the uncertainty of the bias correction, and the statistical noise. A total of 939, 283, and 151 sounding files are available from January 1 to 20 September 2011 at Lindenberg, Cabauw, and Tateno, respectively. The RS92-GDP data have a vertical resolution of 1 s and contain comprehensive metadata, such as the radiosonde type and serial number, the balloon type, the ground-system software version, and the GRUAN data processing version (Immler and Sommer 2011). The amount of corrections applied to the data is also available in the RS92-GDP, and the uncorrected data can be easily recovered.

Our correction method was validated by comparing it with the NCAR GPS PW data (Wang et al. 2007). The GPS PW data have been proven very useful for validating radiosonde humidity data and identifying inhomogeneity in radiosonde records (e.g., Wang and Zhang 2008; Zhao et al. 2012). The GPS-derived PW has an RMS error of less than 3 mm (Wang et al. 2007). The NCAR GPS PW data were reprocessed recently using the new zenith tropospheric delay (ZTD) product from the International Global Navigation Satellite System (GNSS) Service (IGS). The new ZTD product was reprocessed consistently throughout the period with the same approach (Byun and Bar-Sever 2009). Such reprocessing improves the long-term stability of the GPS PW data and enhances its value for climate studies. Eighteen of the RS92 stations shown in Fig. 1 have collocated GPS stations within 50 km horizontally and 100 m vertically. The Lindenberg site is not available in our GPS PW dataset because it is not an IGS site. Instead, the GPS PW data for Lindenberg was obtained from the German Research Centre for Geosciences (GFZ) in Potsdam and are available beginning in December 2009.

### *b. Correcting radiation dry bias*

The Vaisala RS92 humidity sensor has two alternately heated H-HUMICAPS. These sensors are not equipped with the radiation–rain shielding cap installed on the RS80 hygrometer, which makes them more susceptible to solar radiation heating. The heating of the hygrometers and their booms results in a dry bias of the humidity measurement. Different estimates of the RS92 solar radiation dry bias (SRDB) have been made based on comparisons with cryogenic or chilled-mirror frost-point hygrometers (Vömel et al. 2007; Yoneyama et al. 2008; Miloshevich et al. 2009), a microwave radiometer (Cady-Pereira et al. 2008), a Polar Atmospheric Emitted Radiance Interferometer (Rowe et al. 2008), or forecasting models (Agustí-Panareda et al. 2009). These studies found that the magnitude of the SRDB depends on the solar zenith angle, pressure (height), RH, and cloud cover. Many of these studies used other independent measurements as references to develop empirical correction methods, specifically suitable for their own data. In response to the findings of significant SRDB, Vaisala improved the coating of humidity sensor booms to reduce the solar radiation heating in 2006 and 2008 (Vaisala 2011). However, the improvements do not completely remove the SRDB. Therefore, during the eighth WMO Intercomparison of High Quality Radiosonde Systems, held in Yangjiang, China, in July 2010 (Nash et al. 2011), Vaisala introduced a new algorithm to improve humidity measurements. It includes both corrections to the SRDB and the time lag error. The algorithm was shown to greatly improve the RS92 humidity measurements, especially in the upper troposphere and during daytime (Nash et al. 2011). Unfortunately, the Vaisala humidity correction algorithm is proprietary and is not available to users for correcting past Vaisala RS92 data. In the meantime, the new algorithm was implemented in the DigiCORA sounding software version 3.64 in early 2011 and will introduce a discontinuity to the historical radiosonde data at stations where this new software is employed. The radiosonde archive originated from TEMP message sent in real time through the Global Telecommunication System (GTS) does not contain any metadata for this change, and thus the change is not identified and recorded in any operational radiosonde data. To avoid confusion on whether the stations have switched to the new software in early 2011, we only used data up to the end of 2010 for this study. For future work, we plan to use a statistical method and comparisons with other independent data to detect the break points associated with the change implemented in DigiCORA version 3.64. If the Vaisala corrections in DigiCORA

3.64 can be validated, then the last segment of the data where DigiCORA 3.64 was used can be considered as a reference to adjust the historical data.

Researchers may take advantage of the open access of the GRUAN product, its correction algorithm, and its uncertainty estimates. The GRUAN humidity corrections consist of calibration, time lag, and SRDB parts. As shown in the left panel in Fig. 2, total correction (GRUAN, green line) is dominated by the SRDB part (GRUAN\_SRDB, blue line), since on average the sum of the calibration and time lag corrections (GRUAN\_others, light blue line) appears only above 300 hPa and below the tropopause. The calibration error is relatively small, ranging from 0% to 4% in RH at temperatures from 20° to –60°C; thus, it is ignored here. The time lag error is not always systematic because it depends on the RH gradient, the rise rate, and the response time of the hygrometer; thus, it is very sounding specific and its correction requires high-resolution data. As shown later (in Fig. 4), the mean RH difference between NCAR radiation bias correction (NRBC)- and GRUAN-corrected values represents the combined correction for calibration and time and is within 1% on average. For these reasons, we only focus on the SRDB correction.

The GRUAN RS92 SRDB correction is based on the assumption that the heating of the HUMICAPS follows the same laws as the solar heating of the temperature sensor in terms of pressure and ventilation dependence, but with a larger magnitude. The solar radiation heating on the RS92 temperature sensor was measured in Lindenberg using a pressurized box with a fused silica window that holds two RS92 radiosondes, one of which is periodically exposed to the direct radiation from the sun. The other sensor is always in the shadow to serve as a reference. This was repeated frequently, while pressures and ventilation speeds were varied. The heating was calculated from the difference between the exposed and the shadowed sensors. The results show that the heating varies with the solar radiation, pressure, and ventilation speed. These three parameters are independent of the sensor characteristics. Therefore, the heating on the HUMICAPS is assumed to follow the same laws as the temperature sensor but with a larger magnitude because the HUMICAPS does not have reflective coating and is larger. The heating of the HUMICAPS in the GRUAN correction was estimated to be 13 times that of the heating of the temperature sensor. The heating factor of 13 was derived from Eq. (1) by using  $RH_{\text{corr}}$  estimated from the empirical correction in Vömel et al. (2007). Note that in the GRUAN RS92-GDP version 2, the heating factor is 13, 10, and 6.5 for the sondes of batches A and B (manufactured until

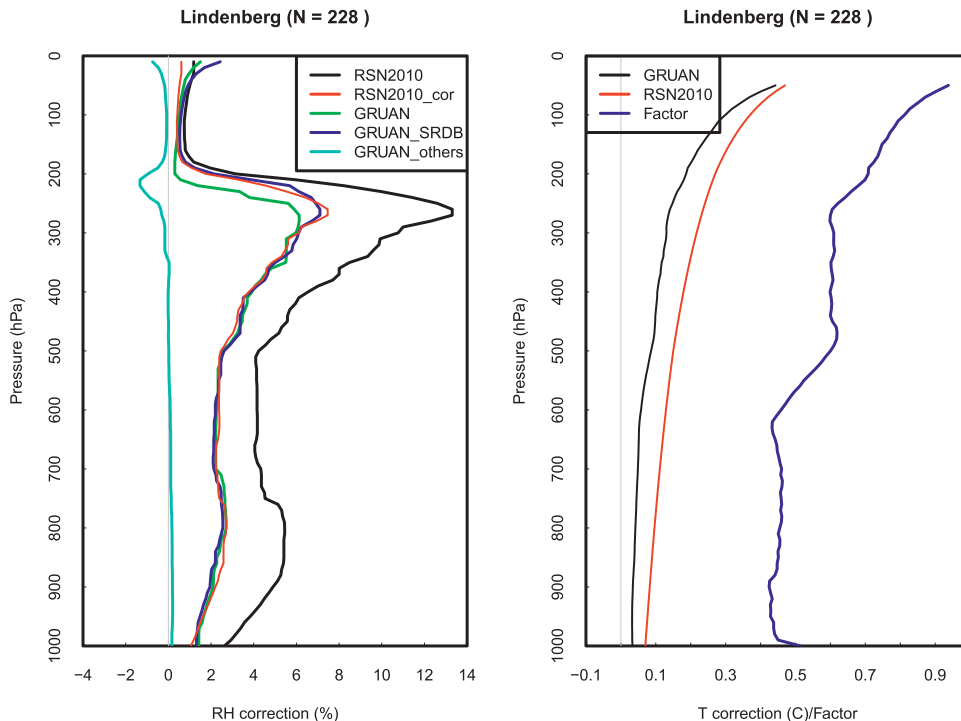


FIG. 2. Comparisons of mean (left) RH and (right)  $T$  corrections from Lindenberg at 1200 UTC using different schemes (see section 2b for details). (left) The RSN2010 and RSN2010\_cor are for SRDB corrections using RSN2010 and adjusted RSN2010 (i.e., NRBC), respectively. The (right) GRUAN and RSN2010 are for GRUAN and RSN2010  $T$  corrections, respectively; also shown is the mean profile of the ratio between GRUAN and RSN2010  $T$  corrections averaged for all data (blue line). The  $N$  in the titles is the number of soundings used in the plots.

2006), C and D (2007 and 2008), and E (2009 and onward), respectively.

Since the radiation flux and ventilation rate are unavailable in global operational radiosonde data used here, one alternative is to use the Vaisala RS92 solar radiation correction table for temperature, released in December 2010 (RSN2010, available online at <http://www.vaisala.com/en/products/soundingsystemsandradiosondes/soundingdatacontinuity/Pages/revisedsolarradiationcorrectiontableRSN2010.aspx>), and to interpolate the correction values to the actual pressures and elevation angles for the data. Figure 2 compares temperature corrections from the GRUAN method and RSN2010 at Lindenberg (similar results for Tateno and Cabauw sites). It clearly shows that the RSN2010 overcorrects the temperature. The same conclusion is drawn from the data at Tateno and Cabauw (not shown). Such overcorrection results in overestimations of RH, especially in the upper troposphere (Fig. 2). It should be noted that although the overcorrection seems quite large (a factor of 2), the magnitude of the solar radiation correction is quite smaller ( $0^{\circ}$ – $0.48^{\circ}\text{C}$  below 50 hPa). The main reason for such an overcorrection is that RSN2010 ignores cloudy

conditions, under which solar radiative heating is reduced, while the GRUAN radiation correction represents the averaged condition of cloudy and clear-sky conditions and bears an uncertainty of  $0^{\circ}\text{C}$ – $0.1^{\circ}\text{C}$ . To minimize the overcorrection, we derived an adjustment factor for the RSN2010 correction using the GRUAN  $T$  correction as a reference. The mean of this adjustment factor increases with decreasing pressures; however, it is approximately independent of pressure and elevation angle within the lower and upper troposphere, with mean values of 0.4 below and 0.6 at or above 500 hPa in the midtroposphere (Fig. 2). Since RH values above 200 hPa are not useful, we did not use a separate value for the layers above 200 hPa, even though Fig. 2 suggests a larger correction factor at these levels. Therefore, the  $T$  correction from RSN2010 is multiplied here by 0.4 below and 0.6 at or above 500 hPa.

The HUMICAP measures the change of the capacitance as a function of water vapor concentration on the thin film sensor (referred to as the response function), which is then converted to RH at the basic calibration temperature by using individual calibration coefficients and then corrected for the temperature

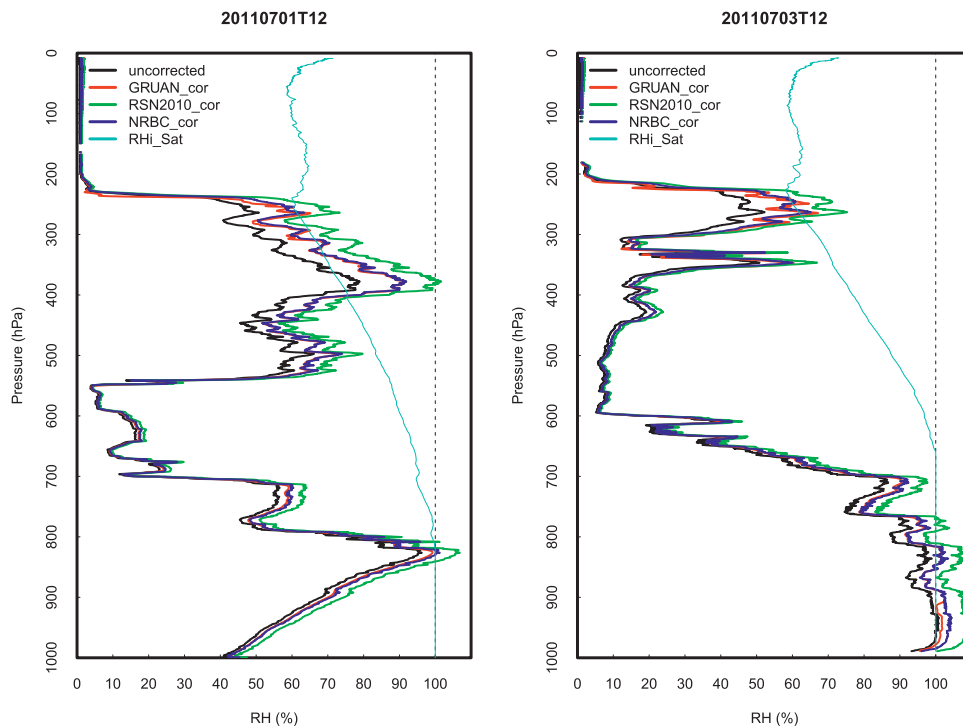


FIG. 3. Comparisons of uncorrected and corrected RH profiles from Lindenberg with different correction schemes applied for two different soundings from Lindenberg. The ice saturation RH is also given (light blue).

dependency of the response function to derive RH at the ambient temperature (Wang et al. 2002; Miloshevich et al. 2009). Because the response function and the temperature dependency correction are unknown, the effect of solar heating on the humidity sensor can be estimated by the effect of the  $T$  warm bias on the saturation vapor pressure since  $RH \approx e/e_s(T)$ , where  $e$  is the vapor pressure and  $e_s(T)$  is the saturation vapor pressure at air temperature  $T$ . Thus, the SRDB-corrected RH ( $RH_{\text{corr}}$  in %) can be calculated as

$$RH_{\text{corr}} = RH_m \frac{e_s(T + hf \times \Delta T_{\text{corr}})}{e_s(T)} \quad (1)$$

where  $RH_m$  is the measured RH (%),  $T$  is the measured air temperature ( $^{\circ}\text{C}$ ),  $hf$  is a heating factor (set to 13), and  $\Delta T_{\text{corr}}$  is the adjusted temperature correction from RSN2010. In (1),  $\Delta T_{\text{corr}}$  is equal to  $cf \times \Delta T_{\text{corr\_RSN}}$ ,

where  $cf$  is the adjustment factor (0.4 or 0.6), and  $\Delta T_{\text{corr\_RSN}}$  is the temperature correction derived from RSN2010. The SRDB correction in Eq. (1) is referred to as the NRBC for relative humidity hereafter. After applying the adjustment to the RSN2010-derived  $T$  correction, the SRDB RH correction from our method agrees very well with the GRUAN correction at all three sites (Fig. 2 for Lindenberg, not shown for the other two sites). Mean RH corrections from NRBC using the data from the three sites vary with pressure and solar elevation angle, and are  $\sim(2\%–4\%)$  (in absolute RH) and 6%–8% in the lower–midtroposphere and upper troposphere, respectively (see Fig. 2 left panel for Lindenberg).

The uncertainty of the NRBC ( $U\_RH_{\text{corr}}$ ) is estimated using Eq. (1) by varying  $\Delta T_{\text{corr}}$  and the heating factor ( $hf$ ) within their standard uncertainties and then taking half of the variations in the RH values as the standard uncertainty as follows:

$$U\_RH_{\text{corr}} = \sqrt{\left( \frac{RH_{\text{corr}, hf=13}^{\Delta T_{\text{corr}} + U_{\Delta T_{\text{corr}}}} - RH_{\text{corr}, hf=13}^{\Delta T_{\text{corr}} - U_{\Delta T_{\text{corr}}}}}{2} \right)^2 + \left( \frac{RH_{\text{corr}, hf=16}^{\Delta T_{\text{corr}}} - RH_{\text{corr}, hf=10}^{\Delta T_{\text{corr}}}}{2} \right)^2} \quad (2)$$

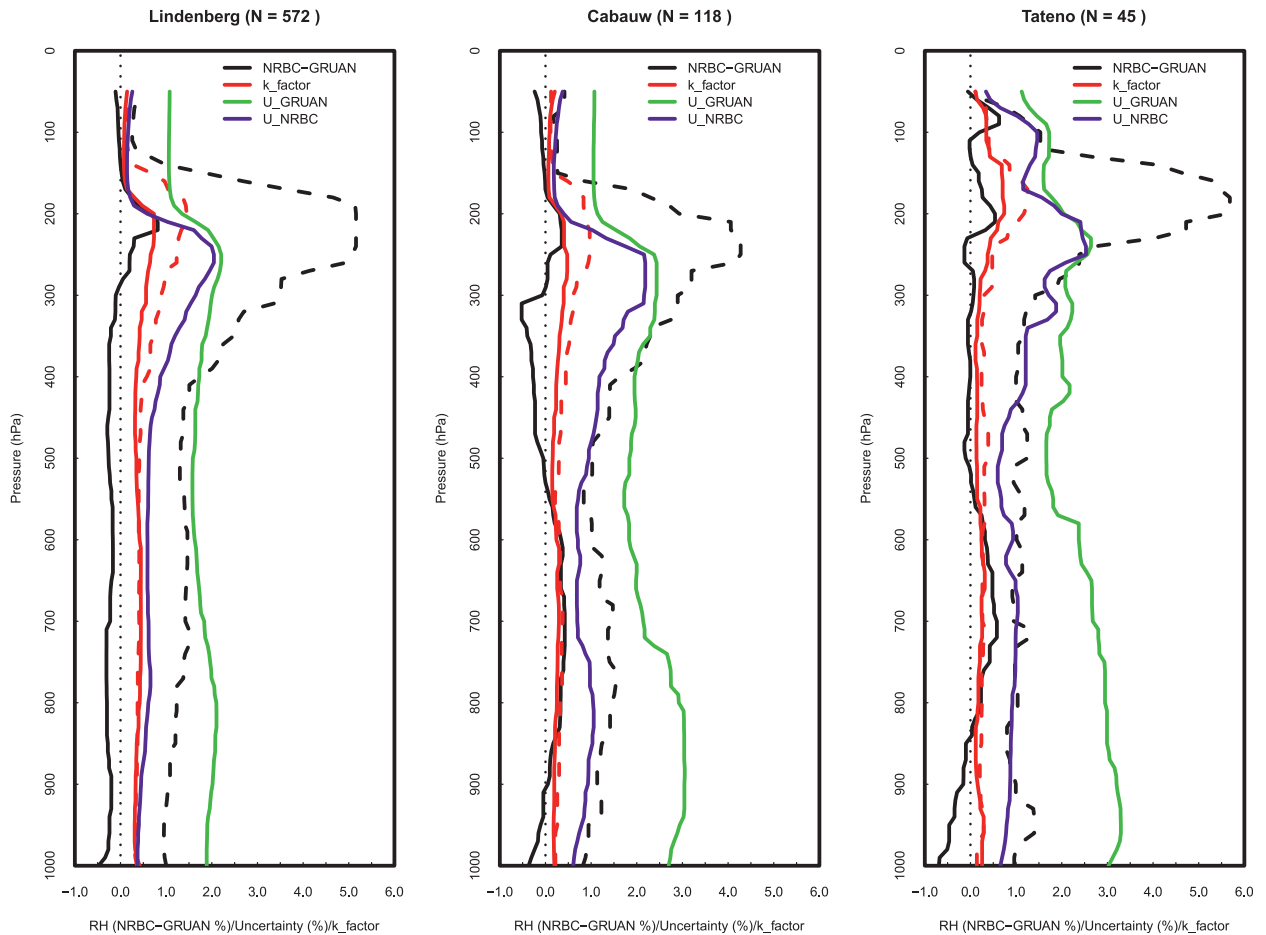


FIG. 4. Vertical profiles of mean (solid lines) and standard deviation (dashed lines) of the RH differences between NRBC and GRUAN corrections (NRBC-GRUAN) and the RH uncertainty for both the NRBC ( $U_{NRBC}$ ) and GRUAN ( $U_{GRUAN}$ ) corrections, and the mean profiles of  $k$  factor (“ $k\_factor$ ”) at three sites for soundings with elevation angles  $> -4^\circ$ . The  $N$  is as in Fig. 2.

$$U_{\Delta T_{corr}} = (U_{cf} + cf \times U_{\Delta T_{corr\_RSN}}) \times T_{corr\_RSN} \quad (3)$$

where  $U_{\Delta T_{corr}}$  is the uncertainty of  $\Delta T_{corr}$ ,  $U_{cf}$  is the uncertainty of the temperature correction factor and is set to 0.1, and  $U_{\Delta T_{corr\_RSN}}$  is the uncertainty of  $\Delta T_{corr\_RSN}$  and is assumed to be 0.05 K. The uncertainty of  $hf$  is 3. The averaged  $U_{RH_{corr}}$  is within 2%, with the largest values in the upper troposphere (see Fig. 4).

### 3. Validation

#### a. Comparisons with GRUAN RS92 corrections

As described in section 2a, the GRUAN RS92 correction addresses calibration, time lag, and solar radiation errors, and it uses a more sophisticated solar radiation correction of the temperature sensor [ $\Delta T_{corr}$  in Eq. (1)] than that used here. The GRUAN correction agrees

well with the Vaisala correction implemented in the DigiCORA software version 3.64, and it has been validated by the cryogenic hygrometer data from the soundings at Lindenberg. Here, we compare uncorrected RH profiles with three corrected versions of the data, using NRBC, RSN2010, and GRUAN corrections. Figure 3 shows two examples at 1200 UTC July 2011 in Lindenberg. The RH corrected using the GRUAN and NRBC are in agreement, while the data corrected using RSN2010 T corrections consistently overestimate RHs, resulting in physically unrealistic values, exceeding 100% (Fig. 3).

Mean profiles of RH differences between the NRBC and GRUAN corrections are within  $\pm 0.5\%$  at the three sites, with standard deviations of  $\sim(1\%–2\%)$  in the lower and midtroposphere and  $\sim(2\%–6\%)$  in the upper troposphere (Fig. 4). One way to test whether NRBC- and GRUAN-corrected RHs are consistent is to utilize the “consistency test” approach presented in

TABLE 1. Terminology for checking consistency between pairs of independent measurements of the same quantity. Variables  $m_1$  and  $m_2$  are independent measurements of the same parameter with standard uncertainties  $u_1$  and  $u_2$ , respectively. The “significance level” indicates the probability of  $|m_1 - m_2| > k\sqrt{u_1^2 + u_2^2}$  occurring (adapted from Immler et al. 2010).

$ m_1 - m_2  < k\sqrt{u_1^2 + u_2^2}$	True	False	Significance level (%)
$k = 1$	Consistent	Suspicious	32
$k = 2$	In agreement	Significantly different	4.5
$k = 3$	—	Inconsistent	0.27

Immler et al. (2010). The consistency ( $k$  factor) is defined in Table 1, where  $u_1$  and  $u_2$  are uncertainties of the two parameters compared, and  $m_1$  and  $m_2$  are measurements of the two parameters. The uncertainty of  $RH_{corr}$  is calculated from Eqs. (2) and (3), and the GRUAN data include RH uncertainty. The mean of the  $k$  factor is  $<1$  for the entire profile, with a standard deviation of  $<1.5$  for all three sites (Fig. 4). This suggests that NRBC-corrected RHs are statistically consistent or in agreement with RHs in the GRUAN data. This is very encouraging and confirms the validity of the NRBC. Note that the uncertainty of the NRBC correction shown in Fig. 4 is smaller than that from the GRUAN. This is because the former only includes the uncertainty of the correction scheme [Eq. (2)], while the RH uncertainty in the GRUAN data is a sum of all sources, including the calibration, radiation, and time lag correction.

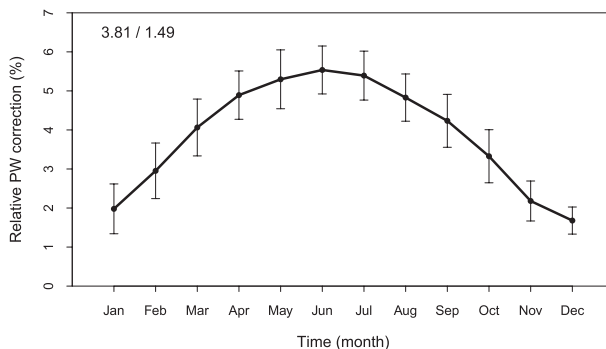


FIG. 5. Seasonal variations of the monthly-mean relative PW corrections at 1200 UTC in Lindenberg. The annual mean and its standard deviation of relative PW corrections are 3.81% and 1.49%, respectively.

*b. Comparisons with GPS PW*

The GPS-derived PW has been used to identify and quantify radiosonde humidity errors (e.g., Wang and Zhang 2008). The impact of the NRBC correction on PW at 1200 UTC in Lindenberg is shown in Fig. 5. The relative PW correction is largest in June, with a mean of  $\sim 5\%$ , and smallest in December, with an average of less than 2%. It implies that the correction would strengthen the PW annual cycle. Compared with the PW derived from ground-based GPS measurements in Lindenberg, the corrections significantly reduce the dry bias, especially for large PW values. The mean dry bias is decreased to 0.49 mm after the corrections compared with 1.1 mm before the corrections (Fig. 6).

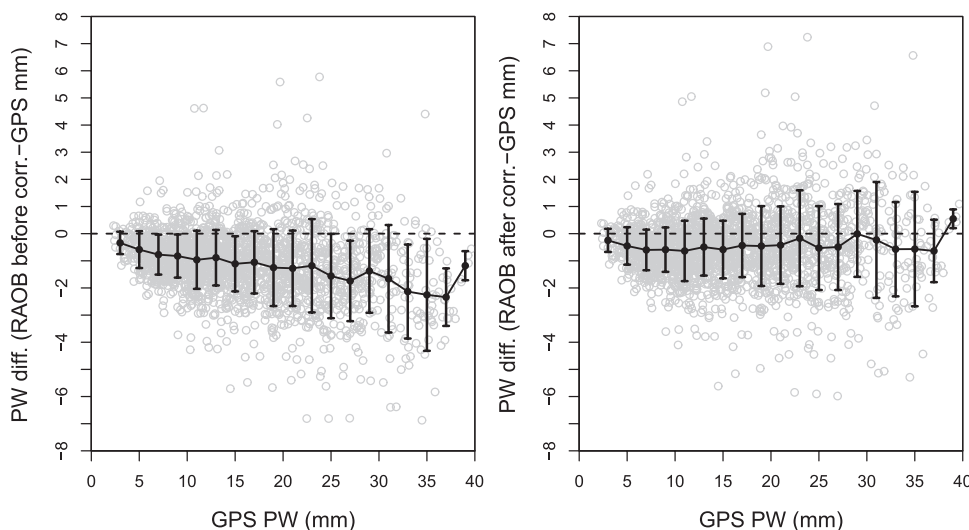


FIG. 6. The PW differences between radiosonde (RAOB) and GPS at 1200 UTC in Lindenberg (left) before and (right) after corrections as a function of the GPS PW. Solid lines and error bars represent the mean and standard deviation of the differences in each bin, respectively.

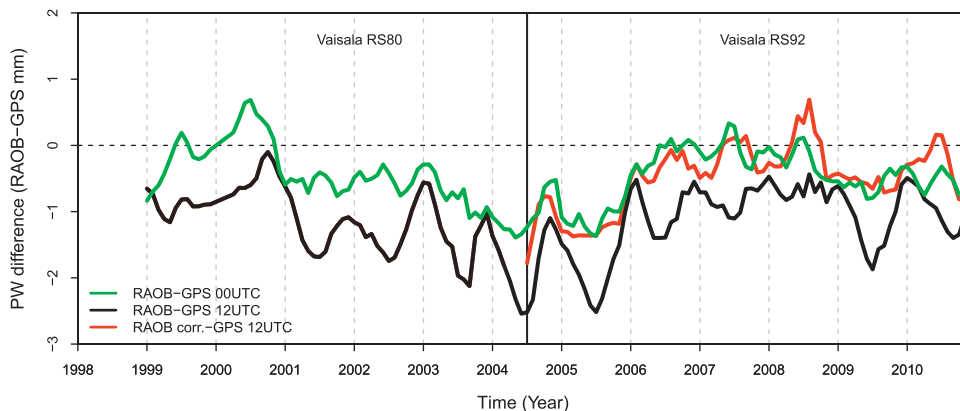


FIG. 7. Time series of the monthly-mean PW differences between the radiosonde and GPS measurements in Lindenberg at 0000 and 1200 UTC for uncorrected (green and black, respectively) and corrected (red) radiosonde data. Note that the correction is not applied to the data at 0000 UTC. Radiosonde types are separated by the vertical black lines and labeled along the top.

Figure 7 shows the time series of the monthly-mean PW differences between the radiosonde (both uncorrected and corrected) and GPS measurements from December 1998 to December 2010 in Lindenberg. During this period, the GPS PW data are available, and Vaisala RS80 and RS92 sondes were launched in Lindenberg. It can be seen that the uncorrected radiosonde PW is consistently lower than that derived from the GPS measurements. The magnitude of the dry bias in the radiosonde data at 1200 UTC (1300 LST) is larger than that at 0000 UTC (0100 LST), and that it has a seasonal variation with larger magnitudes in summer and for RS92. Such dry bias and its characteristics shown in Fig. 7 have been discussed by previous studies (e.g., Wang et al. 2002; Vömel et al. 2007; Wang and Zhang 2008). During the period from July 2004 to December 2010 when the RS92 was used, the dry bias changes with time. This change seems to have resulted from two changes

that Vaisala made to the RS92 humidity sensor to reduce the solar radiation dry bias. In September 2006, Vaisala improved the coating of humidity sensor contacts, which was expected to raise RH values up to 5%–6% larger than those obtained using the old coating (Vaisala 2011). Figure 7 shows that agreement between radiosonde and GPS data was improved after September 2006, although the radiosonde PW is still smaller than the GPS values at 1200 UTC. In June 2008, the back side of the RS92 sensor boom was changed to a shiny silver finish, similar to the front side. Vaisala stated that the effect of such a change was within reproducibility limits based on their test flights (Vaisala 2011). However, Fig. 7 suggests that compared to the previous version, this change introduced a systematic dry bias with a larger magnitude during summer months and at 1200 UTC. The NRBC correction results in better agreement between the radiosonde and GPS data in

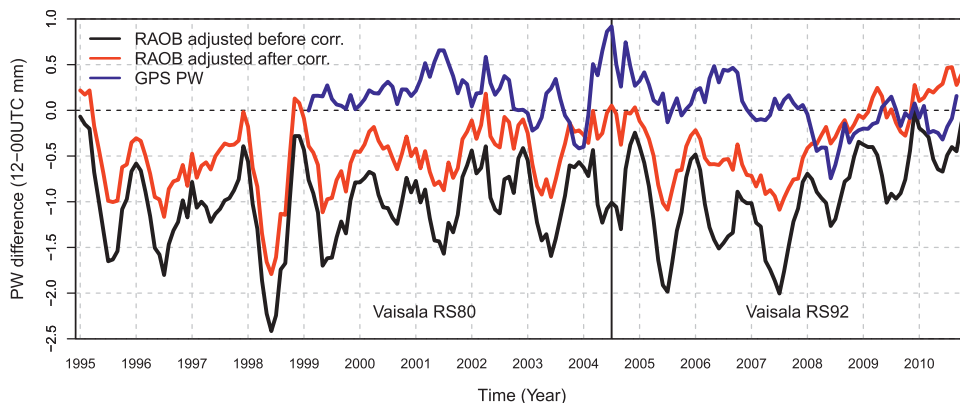


FIG. 8. Time series of the monthly-mean PW difference between 1200 and 0000 UTC from the GPS (blue) and radiosonde data before (black) and after (red) the NRBC. Radiosonde types are separated by the vertical black lines and labeled at the bottom.

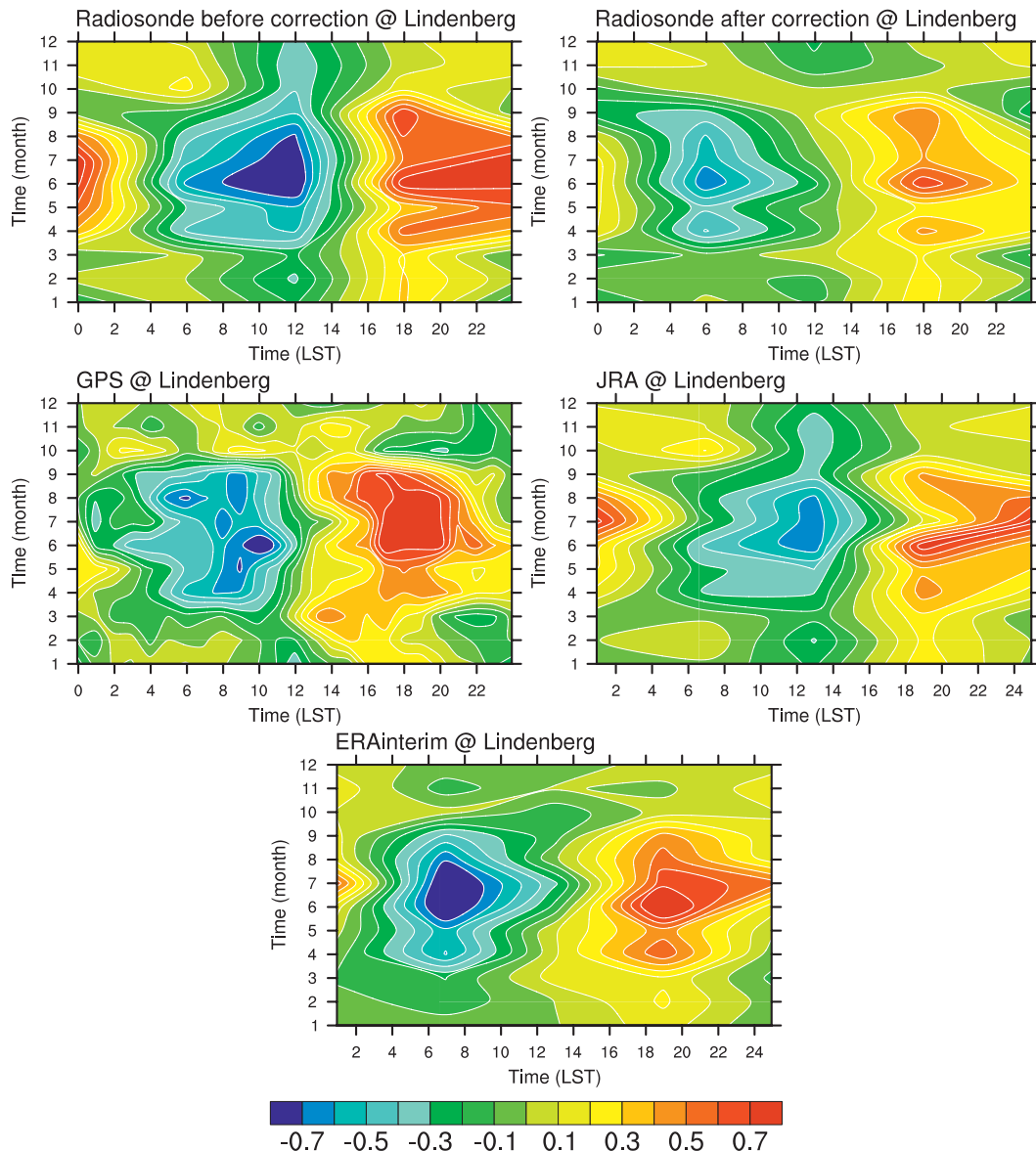


FIG. 9. (top) Seasonal variations of the monthly-mean PW anomalies (mm) at Lindenberg from 6-hourly radiosonde data (before) corrections and (right) after; (middle) (left) hourly GPS PW data and (right) 6-hourly JRA; and (bottom) ERA-Interim products.

summer than in other seasons, and consistent bias characteristics between day and night soundings.

The day and night difference of temperature and humidity is a good measure of the radiation-associated bias. The discrepancy between 1200 UTC [1300 local solar time (LST)] and 0000 UTC (0100 LST) in Lindenberg can be used as a surrogate of the day–night difference (Fig. 8). Without the NRBC correction, Vaisala radiosonde PW is more than 1 mm larger at 0100 LST than at 1300 LST in summer, and both the diurnal difference and seasonal variations are more pronounced for the RS92 data (Fig. 8). This is clearly an artifact of the solar

radiation dry bias in the Vaisala radiosonde data, and as such a diurnal cycle does not exist in the GPS PW data (Fig. 8). After the NRBC correction, the seasonal variability of the day–night difference is reduced and agrees better with the GPS data. These features are more evident in Fig. 9. All three datasets (radiosonde data before and after the corrections, and GPS data) show that a significant diurnal cycle occurs only from April to September. The GPS and corrected radiosonde PW peak around 1700–2000 LST and dip around 0600–1000 LST from April to September; the uncorrected radiosonde data show the peak and dip around midnight and noon,

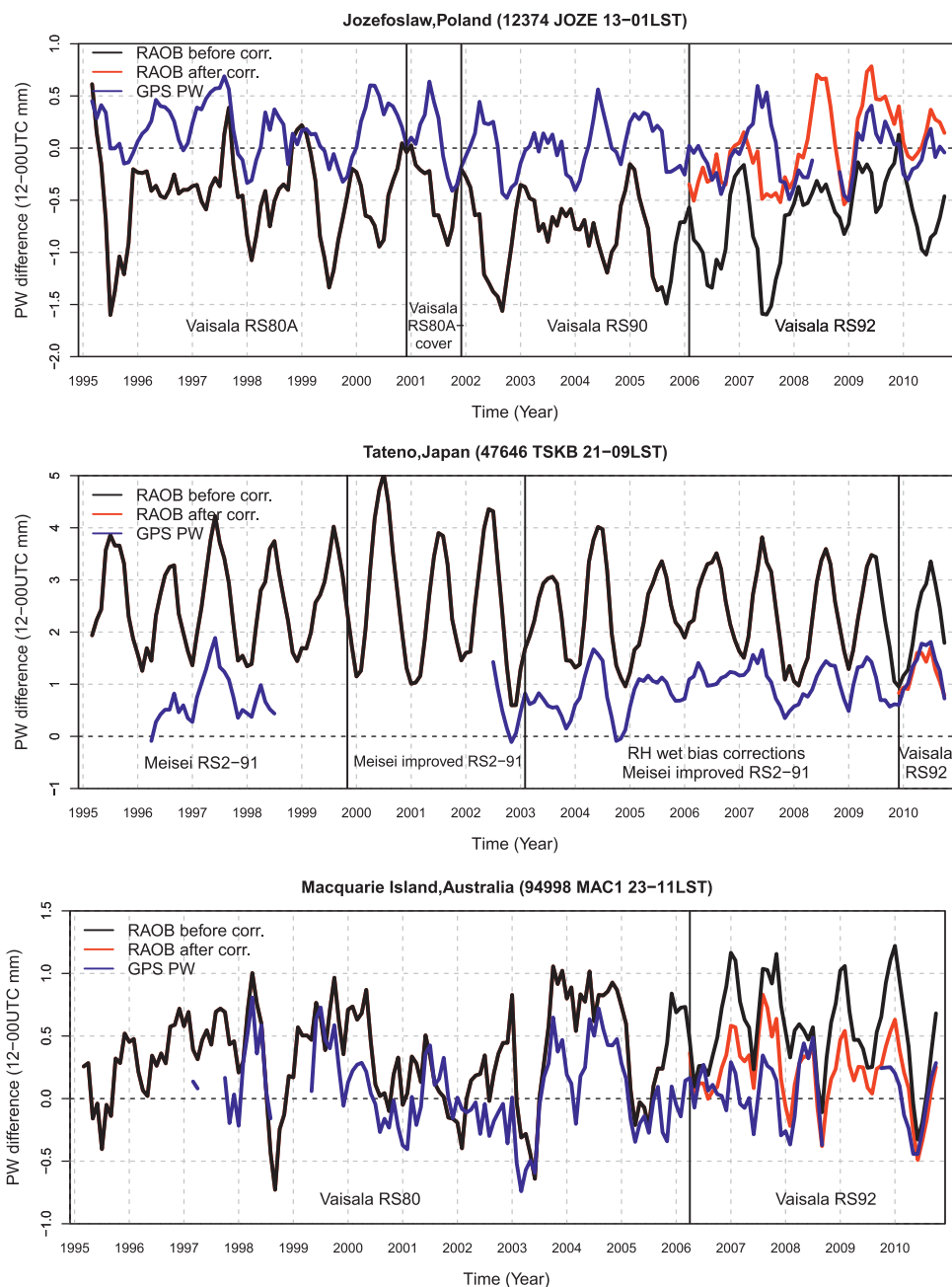


FIG. 10. Time series of the monthly-mean PW difference between 1200 and 0000 UTC from the GPS data (blue) and radiosonde data before (black) and after (red) the NRBC at (top to bottom) three stations. Radiosonde types are separated by vertical black lines and labeled along the bottom.

respectively. In addition, the NRBC correction also leads to weaker PW diurnal cycle (Fig. 9). The Japanese 25-yr Reanalysis (JRA-25) and the European Centre for Medium-Range Weather Forecasts Interim Re-Analysis (ERA-Interim) data during the same period (2004–10) are also shown in Fig. 9. Note that the reanalysis models assimilate uncorrected radiosonde humidity data together with satellite observations. The radiosonde dry

bias is evident in the JRA data; however, the ERA-Interim shows the best agreement with the GPS data. It is unclear what causes the differences between the JRA and ERA-Interim. Both reanalysis products did not assimilate the GPS PW data.

The NRBC was also applied to 17 other stations where GPS stations were closely collocated within 50 km horizontally and 100 m vertically. Various factors

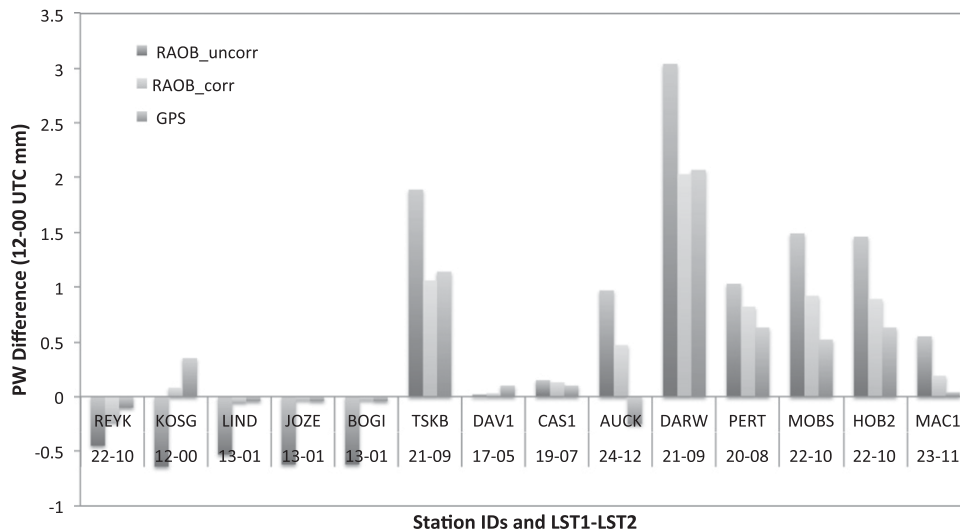


FIG. 11. Mean PW differences between 1200 and 0000 UTC from the GPS and radiosonde data before and after NRBC averaged for the period during which Vaisala RS92 were used at 14 stations. The GPS station names (four letters) and LST1–LST2, where LST1 is the LST for 1200 UTC and LST2 is for 0000 UTC, are given on the horizontal axis.

can contribute to the absolute PW difference between the radiosonde and GPS data, such as differences in measurement techniques, measurement errors, and spatial separations of radiosonde and GPS stations (see discussions in Wang and Zhang 2008). To minimize the contributions from factors other than radiosonde biases, we assumed that the other factors are independent of the time of the day, and then we compared monthly PW differences between 1200 and 0000 UTC for each dataset (GPS data, and radiosonde data before and after the corrections) from 1995 to 2010. Three examples are given in Fig. 10. Similar to the results presented in Fig. 8 for Lindenberg, they clearly show three main features. First, the 1200–0000 UTC PW difference in the radiosonde data varies with radiosonde type. At Józefosław, the magnitude of the PW difference for Vaisala RS90–RS92 is larger than that for Vaisala RS80 as a result of larger dry bias for the twin HUMICAP used for RS90–RS92 at 1200 UTC (1300 LST). At Tateno, the 1200–0000 UTC PW difference is very large and has strong seasonal variations; its magnitude decreases in summer after 2003, when the RH wet bias correction was applied to the Meisei RS2-91 data at temperatures colder than 0°C for both day and night soundings (Ishihara 2004). At Macquarie Island, the 1200–0000 UTC PW difference in the RS92 data displays more regular seasonal variations and larger values in summer than those in the RS80 data. Second, the 1200–0000 UTC PW difference generally shows larger and more regular seasonal variations in the radiosonde data than in the GPS data. Last, they all show improved agreements with the GPS data after the

NRBC. Such improvement is seen for all other sites with twice-daily data as shown in Fig. 11 for averaged 1200–0000 UTC PW differences. Note that only 14 sites are shown in Fig. 11 after removing three sites where the data are not available at either 0000 or 1200 UTC. After the NRBC, the absolute mean 1200–0000 UTC PW difference at all 14 sites is decreased in the radiosonde data and corresponds better with the GPS data (Fig. 11). Mean differences between the radiosonde (both uncorrected and corrected) and GPS in the 1200–0000 UTC PW for each station are computed. Then the mean and RMS of them over all stations are calculated, and are  $0.19 \pm 0.71$  and  $0.08 \pm 0.25$  for uncorrected and corrected radiosonde data, respectively.

#### 4. Impact on homogenized humidity data

As stated in section 1, one of the primary objectives for this study is to improve the homogenized long-term radiosonde humidity data. We first applied the NRBC correction to historical radiosonde data for years when RS92 sondes were used, and then we homogenized the entire data series using the method explained in Dai et al. (2011). Figure 12 shows the impact of the NRBC on the time series of monthly-mean RH at 1200 UTC at different levels in Lindenberg. The inhomogeneity of the RH time series in the raw data (black lines in Fig. 12) is apparent in 1993, and it results from a change in sensor manufacturer from the Union of Soviet Socialist Republics (USSR) Mars radiosondes to Vaisala radiosondes. The USSR Mars radiosondes used

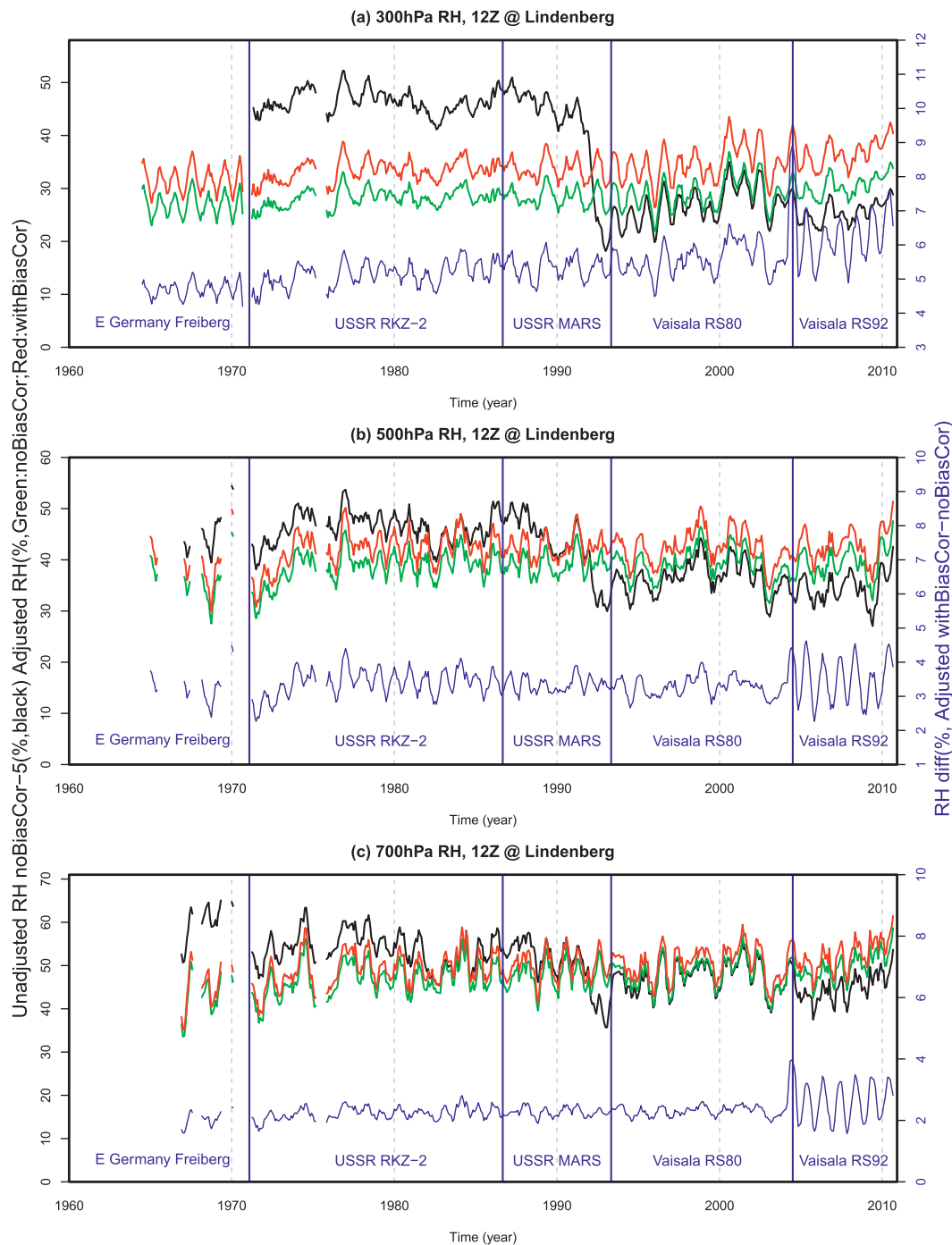


FIG. 12. Monthly time series of the raw (black) and homogenized (colors) RH (%) for 1200 UTC at (a) 300, (b) 500, and (c) 700 hPa at Lindenberg. The red and green lines are cases with and without the NRBC, respectively. The blue line is the difference between the homogenized, or adjusted, data with and without the NRBC. Vertical blue lines divide different radiosonde types, labeled along the bottom. Note that the unadjusted data (black curves) have been intentionally shifted downward by 5% in order to make them more visible.

Goldbeater’s skin for humidity measurements and had a slow response, resulting in a wet bias of the measurements. Such a wet bias is especially pronounced at higher altitudes, where air temperature is low and the

RH vertical gradient is large. The homogenization successfully removed the discontinuity observed in 1993 and made the time series more consistent (green lines in Fig. 12). The adjustment in the time series uses the last

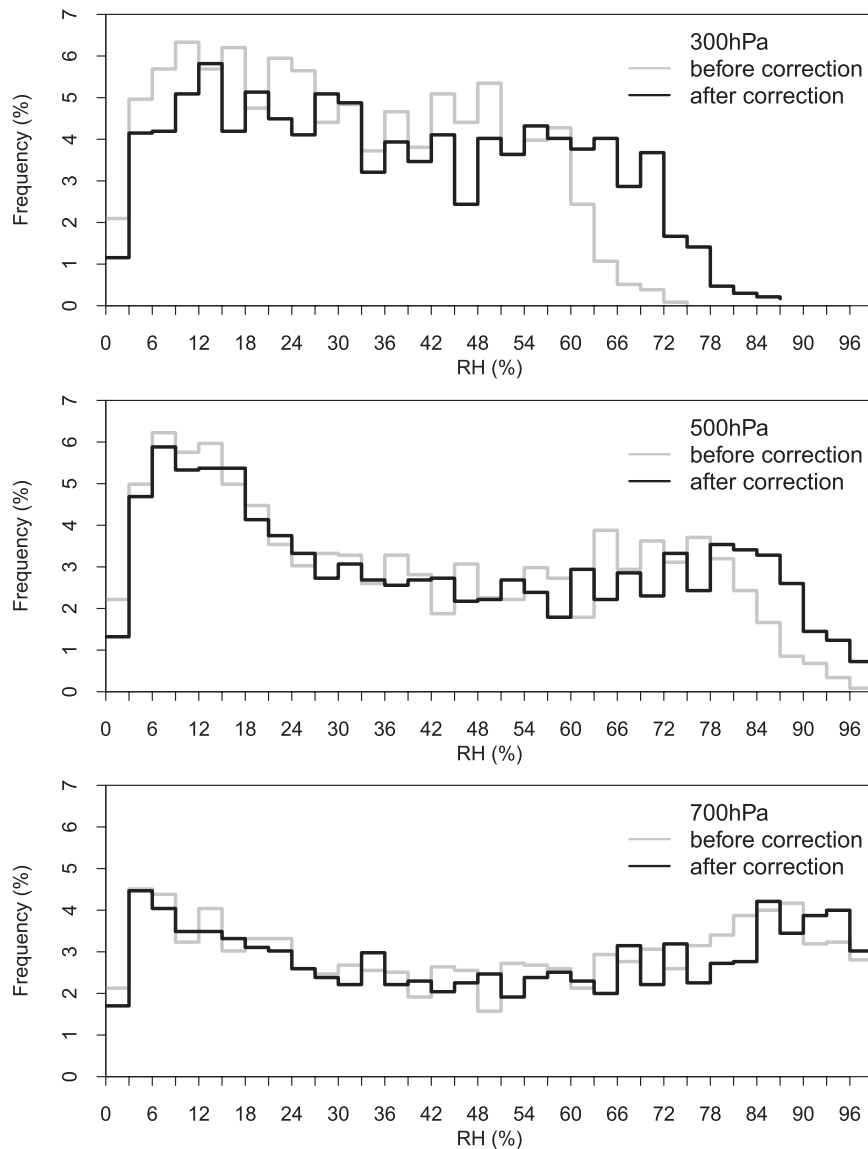


FIG. 13. Histograms of RH for 1200 UTC at (top to bottom) 300, 500, and 700 hPa in Lindenberg for the last segment before (gray) and after (black) the NRBC.

segment as the reference when Vaisala RS92 was used. As described above, the RS92 data contain a daytime radiation dry bias that requires correction. Therefore, the last segment of the raw data was first subjected to the NRBC, and then it was used to adjust the data in other segments (red lines in Fig. 12). Compared with the homogenized time series with and without the bias correction, the NRBC increases the RH mean values by 5.3%, 3.3%, and 2.3% at 300, 500, and 700 hPa, respectively, with larger corrections at higher altitudes. The bias correction shifts the entire record, although it was only applied directly to the last segment (after April 2004). The increase is relatively constant with time (blue

lines in Fig. 12), although it has weak seasonal variations in early segments. Dai et al. (2011) used a DPD quantile-matching algorithm to adjust the time series so that the earlier segments have DPD histograms comparable to that of the latest segment. However, the quantile matching was not done separately for each season because of limited sample size. As a result, the large seasonal variation of the corrections in the last segment was not fully kept for earlier segments. Figure 13 shows the RH histograms at 300, 500, and 700 hPa in Lindenberg for the cases with and without the NRBC. The NRBC significantly increases the occurrence frequency for large RH values, implying more saturation cases in the

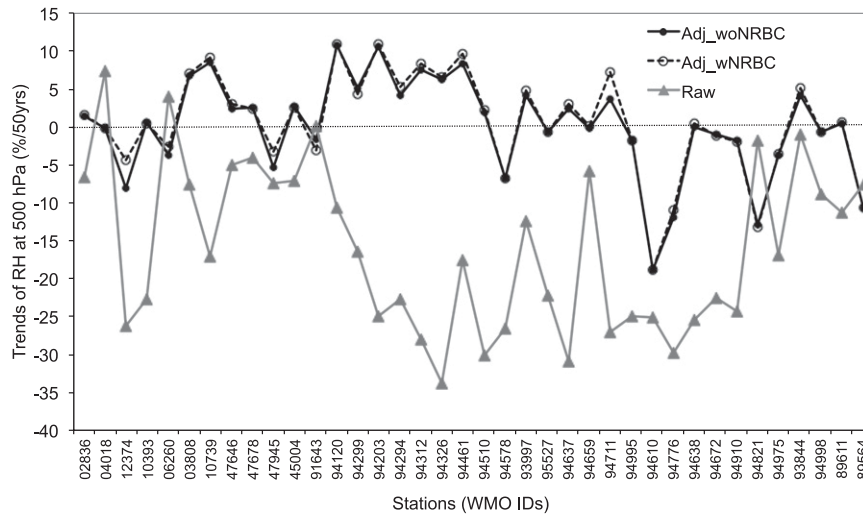


FIG. 14. The RH trends from 1970 to 2010 [ $\% (50 \text{ yr})^{-1}$ ] of raw and homogenized data, with and without the NRBS at 500 hPa from 38 stations.

bias-corrected data. Similar features were seen at other stations. Mean RH corrections averaged over all 65 stations that used the RS92 sondes and the entire data record are 2.9%, 1.7%, and 1.5% at 300, 500, and 700 hPa, respectively. In summary, the NRBC changes the mean state of the atmosphere for the entire data period; thus, it could have significant impacts on other related fields when the uncorrected data are assimilated into reanalysis models.

The impact of the NRBC on the trends is examined by comparing long-term RH trends from the raw data and homogenized data with and without the NRBC at 38 stations where at least 10 years of data are available for trend analysis (Fig. 14). The raw data produce large negative RH trends as a result of moist biases in early years because of the slow response of old types of hygrometers. Such a characteristic is most pronounced for Australian stations [World Meteorological Organization (WMO) Identification (ID) starting with “94”]. The homogenization greatly reduces the trends and makes them more spatially consistent. The NRBC has very little impact on the trends. This is not surprising because the bias correction is roughly constant with time as shown in Fig. 12. However, it should be kept in mind that our goal is to not only obtain the best estimate of long-term trends but also to obtain the most accurate estimate of the humidity values for global reanalysis applications.

The impact of the NRBC on the PW diurnal cycle for the RS92 data can be extended to the data for the entire period after the homogenization is applied. The NRBC reduces the 1200–0000 PW difference and its seasonal variation and improves its agreements with the GPS PW data for the whole data period at Lindenberg and Macquarie Island (Fig. 15). A plot similar to Fig. 11 is

also made of the data over the whole time series for adjusted radiosonde data with and without NRDB corrections. Better agreements with the GPS data are achieved for corrected data, but the improvement is not as large as what is shown in Fig. 11. This is due to interannual variations of PW 1200–0000 differences, different time periods for GPS and radiosonde data, and different characteristics in diurnal biases for the early radiosonde types. The more realistic PW diurnal cycle in the bias-corrected radiosonde data could potentially improve the water vapor diurnal cycle in future reanalysis products and this could lead to an improved representation of the precipitation diurnal cycle in reanalyses.

## 5. Conclusions

Vaisala RS92 is the most widely used radiosonde type in the current global network ( $\sim 30\%$  of the stations). Considerable efforts have been made to study the systematic errors in RS92 humidity data. One of the most significant biases is its daytime solar radiation dry bias (SRDB) due to the heating of the sensor boom. This bias also introduces inhomogeneity to historical radiosonde records. This study represents the first attempt at developing and validating a physically based algorithm to correct the SRDB in historical radiosonde RH data. Our algorithm, referred to as NRBC, is based on a more complicated GRUAN algorithm, but it has been simplified to make it applicable for operational data without any information on the solar radiation flux and rise rate. The correction was derived by assuming that the solar heating of the HUMICAPS follows the same principle of the temperature sensor, but it has a much larger (13 times) magnitude. The solar heating of the temperature

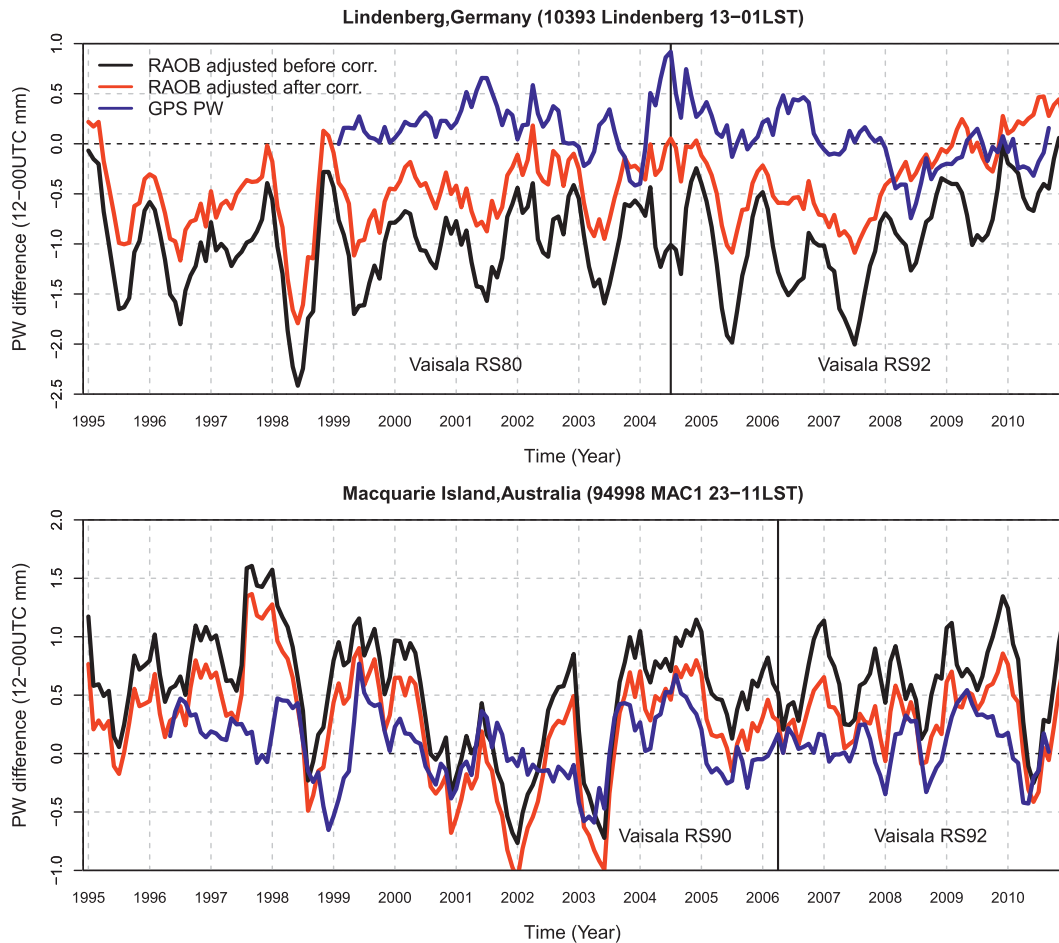


FIG. 15. Time series of the monthly-mean PW difference between 1200 and 0000 UTC from the GPS (blue) and homogenized (adjusted) radiosonde data before (black) and after (red) the NRBC at (top to bottom) two stations.

sensor was estimated using the correction table for clear-sky conditions provided by the manufacturer and is a function of the air pressure and solar elevation angle. To account for cloudy conditions, the solar heating correction is reduced by a factor of 0.4 below and 0.6 at or above 500 hPa. The temperature correction factor was derived from comparisons with the more highly accurate GRUAN temperature correction. The NRBC [Eq. (1)] is dependent on measured RH and temperature and the solar radiation correction for temperature. Based on the data from three GRUAN sites, the RH corrections vary with pressure, season, and the time of the day, have a mean magnitude of  $\sim(2\%–4\%)$  in the lower and midtroposphere, and increase to 6%–8% in the upper troposphere. The uncertainty of the NRBC [Eq. (2)] is also estimated to be within 2%, with the largest values in the upper troposphere.

The NRBC was evaluated against the GRUAN RS92 corrections and the PW estimated from ground-based

GPS measurements. The NRBC-corrected RH is statistically in agreement with the corrected RH from the GRUAN dataset. The NRBC leads to a reduced bias compared with the GPS PW data, and is in better agreement with the GPS PW diurnal cycle in both phase and amplitude. It also improves the temporal homogeneity of the 1200–0000 UTC PW difference time series for the radiosonde data, when compared with the GPS data. The diurnal biases in radiosonde humidity data can introduce spurious diurnal variations; thus, caution must be taken when using the raw radiosonde data to study diurnal variations. The homogenized data record shows increased RH values throughout the entire record, although the NRBC is only applied to the last segment of the time series, where RS92 radiosonde data were collected. However, the NRBC has negligible impacts on long-term RH trends.

The NRBC has several limitations in spite of the positive impacts discussed above. First, the clear-sky and

cloudy conditions and their variations with height for each sounding are not considered in the NRBC. Rather a constant factor (0.4 or 0.6) multiplies the RSN2010 temperature correction. As a result, it leads to over-correction of the RH values inside clouds and likely undercorrection in some cases for clear-sky conditions. Some recommendations for the future that may help resolve this would be collection of metadata about cloudy conditions (clear–cloud and cloud types), future radiosonde development involving small and cost-effective radiation sensors to fly with the standard radiosondes, and installing a temperature sensor near the humidity sensor to accurately measure the heating. Current surface synoptic data include some cloud information, which would be useful for improving the correction algorithm described here. However, it is important to incorporate the cloud information at the radiosonde launch location and time and during the flight in the radiosonde data. Second, the ventilation rate is not taken into account for the solar heating in the NRBC because of the lack of availability of the balloon rise rate in the data, given the Vaisala radiation correction formula's dependence on the rise rate. We strongly recommend that future operational radiosonde reports include balloon rise rates, and the manufacturers should openly disclose all correction algorithms applied to the final data products. Third, a constant factor of 13 is used here to account for larger solar heating for humidity sensors than for temperature sensors. This factor varies in the improved GRUAN correction for GRUAN RS92-GDP version 2 depending on the sonde batch corresponding to Vaisala's modifications to the sensor boom (discussed in section 2b). This cannot be applied to the operational data because the sonde batches are unknown. Finally, while it is encouraging that the manufacturer (Vaisala, in this case) has made efforts to improve the RS92 humidity measurements by improving both hardware (sensor boom modifications) and software (Vaisala RS92 corrections), these changes introduce a discontinuity into the global radiosonde record, especially when they are not well documented. As a result, they cannot be easily identified and adjusted. Additionally, the unavailability of the Vaisala correction algorithm prohibits its application to past radiosonde dataset. To maintain a high-quality climate record from either the operational radiosonde network or the GRUAN network, it is essential for the manufacturers to freely disclose all correction algorithms and to collaborate with researchers to better manage change.

*Acknowledgments.* This work was supported by NOAA (Grant NA10OAR4310056). We thank Güldner

Jürgen from DWD and GFZ Potsdam for providing the Lindenberg GPS PW data, and Zaihua Ji and Steve Worley at NCAR CISL for archiving GPS data. We would also like to acknowledge Kathryn Young's and Scot Loehrer's constructive comments on the manuscript.

## REFERENCES

- Agusti-Panareda, A., and Coauthors, 2009: Radiosonde humidity bias correction over the West African region for the special AMMA reanalysis at ECMWF. *Quart. J. Roy. Meteor. Soc.*, **135**, 595–617.
- Byun, S. H., and Y. E. Bar-Sever, 2009: A new type of troposphere zenith path delay product of the international GNSS service. *J. Geod.*, **83**, 367–373.
- Cady-Pereira, K. E., M. W. Shephard, D. D. Turner, E. J. Mlawer, S. A. Clough, and T. J. Wagner, 2008: Improved daytime column-integrated precipitable water vapor from Vaisala radiosonde humidity sensors. *J. Atmos. Oceanic Technol.*, **25**, 873–883.
- Ciesielski, P. E., and Coauthors, 2010: Quality controlled upper-air sounding dataset for TiMREX/SoWMEX: Development and corrections. *J. Atmos. Oceanic Technol.*, **27**, 1802–1821.
- Dai, A., J. Wang, P. W. Thorne, D. E. Parker, L. Haimberger, and X. L. Wang, 2011: A new approach to homogenize daily radiosonde humidity data. *J. Climate*, **24**, 965–991.
- Durre, I., R. S. Vose, and D. B. Wuertz, 2006: Overview of the Integrated Global Radiosonde Archive. *J. Climate*, **19**, 53–68.
- Immler, F. J., and M. Sommer, 2011: Brief description of the RS92 GRUAN data product (RS92-GDP). GRUAN Tech. Document GRUAN-TD-4, 17 pp. [Available online at <http://www.gruan.org/>]
- , J. Dykema, T. Gardiner, D. N. Whiteman, P. W. Thorne, and H. Vömel, 2010: A guide for upper-air reference measurements: Guidance for developing GRUAN data products. *Atmos. Meas. Tech. Discuss.*, **3**, 1217–1231, doi:10.5194/amt-3-1217-2010.
- Ishihara, M., 2004: Recent tests and comparisons of radiosonde operated by Japan Meteorological Agency. WMO Document CIMO/OPAG-UPPER-AIR/ET-UASI-1/IOC-1/Doc. 3.2(3), 8 pp.
- Miloshevich, L. M., H. Vömel, D. N. Whitman, and T. Leblanc, 2009: Accuracy assessment and correction of Vaisala RS92 radiosonde water vapor measurements. *J. Geophys. Res.*, **114**, D11305, doi:10.1029/2008JD011565.
- Nash, J., T. Oakley, H. Vömel, and W. Li, 2011: WMO intercomparisons of high quality radiosonde systems. WMO Tech. Doc. WMO/TD-1580, Instruments and Observing Methods Rep. 107, 238 pp. [Available online at [http://www.wmo.int/pages/prog/www/IMOP/publications/IOM-107\\_Yangjiang.pdf](http://www.wmo.int/pages/prog/www/IMOP/publications/IOM-107_Yangjiang.pdf)]
- Nuret, M., J.-P. Lafore, F. Guichard, J.-L. Redelsperger, O. Bock, A. Agusti-Panareda, and J.-B. N'Gamini, 2008: Correction of humidity bias for Vaisala RS80-A sondes during the AMMA 2006 observing period. *J. Atmos. Oceanic Technol.*, **25**, 2152–2158.
- Rowe, P. M., L. M. Miloshevich, D. D. Turner, and V. P. Walden, 2008: Dry bias in Vaisala RS90 radiosonde humidity profiles over Antarctica. *J. Atmos. Oceanic Technol.*, **25**, 1529–1541.

- Seidel, D. J., and Coauthors, 2009: Reference upper-air observations for climate: Rationale, progress, and plans. *Bull. Amer. Meteor. Soc.*, **90**, 361–369.
- Vaisala, cited 2011: Sounding data continuity. [Available online at <http://www.vaisala.com/en/products/soundingsystemsandradiosondes/soundingdatacontinuity/Pages/default.aspx>.]
- Vömel, H., and Coauthors, 2007: Radiation dry bias of the Vaisala RS92 humidity sensor. *J. Atmos. Oceanic Technol.*, **24**, 953–963.
- Wang, J., and L. Zhang, 2008: Systematic errors in global radiosonde precipitable water data from comparisons with ground-based GPS measurements. *J. Climate*, **21**, 2218–2238.
- , H. L. Cole, D. J. Carlson, E. R. Miller, K. Beierle, A. Paukkunen, and T. K. Laine, 2002: Corrections of humidity measurement errors from the Vaisala RS80 radiosonde—Application to TOGA COARE data. *J. Atmos. Oceanic Technol.*, **19**, 981–1002.
- , L. Zhang, A. Dai, T. Van Hove, and J. Van Baelen, 2007: A near-global, 2-hourly data set of atmospheric precipitable water from ground-based GPS measurements. *J. Geophys. Res.*, **112**, D11107, doi:10.1029/2006JD007529.
- Yoneyama, K., M. Fujita, N. Sato, M. Fujiwara, Y. Inai, and F. Hasebe, 2008: Correction for radiation dry bias found in RS92 radiosonde data during the MISMO field experiment. *SOLA*, **4**, 13–16, doi:10.2151/sola.2008-04.
- Zhao, T., A. Dai, and J. Wang, 2012: Trends in tropospheric humidity from 1970 to 2008 over China from a homogenized radiosonde dataset. *J. Climate*, **25**, 4549–4567.